Dry-sliding wear of laser clad nickel aluminide / chromium carbide coatings against cast iron

Sven Bengtsson[a], Senad Dizdar[a], and Karin Gong[b]
[a)] Höganäs /S/, [b)] Göteborg /S/

International Thermal Spray Conference,
June 7-9, Düsseldorf, Germany

The wear of piston rings in large marine two-stroke diesel engines is a major maintenance cost. Applying coatings with good oxidation, corrosion resistance and high temperature strength, can lower the total maintenance cost. In the past nickel aluminide with chromium carbide have been applied to pistons by thermal spraying. Using laser cladding a suitable microstructure can be formed while at the same time avoiding cracks and bonding issues. In this report powders and coatings were manufactured in order to be able to investigate the dry-sliding wear behavior. Material with three levels of carbides was atomized. Wear test samples were manufactured by laser cladding. The dry sliding wear-mechanism maps are generated by using block on ring test setup where coated blocks slide against cast iron rings. All alloys exhibited regions of plasticity-dominated wear and oxidational wear with a transition region in-between. The carbide-containing alloys showed lower friction and wear in comparison to the carbide free nickel aluminide alloy.

1. Introduction

The requirements on modern marine diesel engines are becoming higher and higher. The requirement for high power to volume ratio is higher than ever, combined with the ability to run long periods at reduced power and the need to burn low-sulfur fuels [1] in order to reduce environmental pollution [2]. Furthermore, the need for longer service intervals and higher availability is also strong.

Accordingly, piston rings of marine diesel engines are getting increased severity of the working conditions. Sulphur and its compounds are known to act as anti-wear and extreme pressure additives to lubricating oils. These additives forms thin friction and wear reducing boundary layers-films able to separate the contacting surfaces in boundary and mixed lubrication regimes when full oil film lubrication cannot be established or can fail [3]. Reduction in sulfur amount in the diesel fuel, reduces significantly the sulfurs ability to form the protective boundary layers. .

The risks for severe wear of piston rings are highest near the piston top dead center position when high gas pressure, high temperature and low sliding speed do not allow establishing of full oil lubricating film. Further down the piston stroke, the sliding speed increases, and the temperature drops which is beneficial for establishment of full oil film lubrication regime and leads to minimal risks for wear of the piston rings..

Piston rings for large two-stroke marine diesel engines are subjected to wear and corrosion during operation limiting the usable service interval. By extending the life time of the piston rings the service intervals can be increased and total maintenance costs decreased. This improvement can be achieved by using coatings on the piston rings [4–8]. Hard chrome plating was one of the first methods used to improve wear performance of the piston ring [4]. Other widespread methods are plasma spray and high velocity oxy-fuel spray (HVOF) coatings [9]. Other friction reducing materials, such as $MoSi_2$ has also been used [10]. In some cases the thermal spray methods, such as HVOF, cannot achieve enough strong bonding to the substrate or inside the deposited layer. This can result in increased wear rates [9].

An interesting material combination is nickel aluminide [11,12] combined with chromium carbide [13]. This material combination has been applied as a coating using plasma spray and high velocity oxy-fuel coating processes [5,6,10]. The intermetallic Ni_3Al-based alloys are promising candidates for developing high-temperature and high-strength materials in wear-resistant applications [11,12,14]. This group of alloys exhibit two attractive engineering properties their increasing yield strength with increasing temperature up to about 650ºC -750 ºC and the ability to resist oxidation and corrosion at high temperature [15].

The reinforcing phase, chromium carbide exists in different forms; Cr_3C_2, M_7C_3, $M_{23}C_6$ where M is Cr, Fe, or possibly other metals if available. Typically, the hardness is highest for the Cr_3C_2 carbide followed by M_7C_3, and $M_{23}C_6$. If Cr_3C_2 carbide particles is mixed with nickel aluminide and subsequently welded, the carbide will dissolve quickly in the melt and re-precipitate on solidification. However, depending on amount of Cr_3C_2 added to the mix it will precipitate as one or two of the possible carbides. If the total concentration of carbon is, low it will precipitate as $M_{23}C_6$ and if it is high, it will form Cr_3C_2. However, it is also possible to form graphite if the carbon concentration is too high. A complicating factor is that chromium is a required alloying element in the nickel aluminide matrix. In the present concentration regime for the matrix two phases can form NiAl and Ni_3Al. The amount of NiAl should be kept at low levels since the NiAl is brittle at room temperature and exhibit moderate strength and hardness at high temperature. However, it can be used to buffer the composition and to allow impurities to accumulate in this phase rather than precipitate on grain boundaries since the Ni_3Al does not dissolve typical impurities at all.

Alloys were atomized in the pilot scale atomizer at Höganäs AB, Sweden. The compositions were selected based on the discussion above and the guidelines in previous work [16]. Three compositions are included in this investigation, based on amount of carbide in the alloy. Without carbides the general hardness is expected to be too low for sufficient wear performance, while with too much carbide the weldability will be insufficient, with extensive cracking as result. By this approach it was expected to have a good characterization of the wear behavior of this alloy system in terms of tribological behavior.

The powder is used for laser cladding of wear test blocks for block on ring adhesive dry testing. The rings are made of a cast iron similar to cylinder liner material for large marine diesel engines. The wear tests are performed in dry – unlubricated conditions, at two load and five sliding velocity levels in order to simulate the variety of speeds that the piston ring encounter during its cycle.

The aim of this work is to investigate-rank the dry-sliding friction and wear of nickel aluminide alloys with chromium carbide in a model wear test designed to rank adhesive wear of materials aimed for the piston ring / cylinder liner application.

2. Experimental

The materials were atomized in the Pilot scale gas atomizer and sieved to 53 – 150 micrometer sieve cut. The chemical composition is found in Table 1. The atomized powders were basically spherical with few satellites or other geometrical distortions.

Table 1. Chemical composition of the tested powders.

Code	Composition (wt.%)						
	C	B	Ni	Fe	Cr	Al	Other
A	2.5	0.03	bal		30,4	9,5	
B	6.3	0.18	bal	5,6	43,5	4,6	0.3Mn, 0.3Ti
C	-	0.04	bal	11,1	8,4	10,5	

The laser cladding was performed using an IPG 6 kW fiber coupled diode laser with a Coax 8 powder feed nozzle and a 5 mm round spot. The determination of the process window was typically performed using two to three laser travel speeds a powder feed rate designed to give approximately 1 mm thick single track coating and a variation of laser power in order to reach a modest dilution (target 2-10%) without significant interface or inter track porosity. The dilution is defined as the area fraction of melted substrate divided by the area sum of melted substrate and coating. In some cases pre-heating of the substrate was required in order to avoid welding cracks. In most cases the samples were allowed to cool in vermiculite until the temperature is below 50 ^{o}C. Once suitable parameters are found using the single track samples wear test plates are clad using several adjacent tracks with a defined overlap between tracks. The clad samples were examined visually for defects and by liquid penetrant testing for surface cracks. The porosity and the dilution was examined by light optical microscopy of the as polished surface on cross sections of single track coatings. The interface and inter track porosity is also examined on the wear test samples. A more detailed metallographic investigation was performed using a Hitachi SU6600 FEGSEM scanning electron microscope equipped with a Bruker energy dispersive spectrometer.

In Fig. 1 an example of defining the process window for the laser cladding process is given. Here it can be seen at laser power above 3 kW no interface porosity is found, thus ensuring good fusion. At a laser power of 4 kW the dilution is 5%. Acceptable limit of interface porosity is below 0.1% while dilution should be between 2 and 5%. The process window for material A is a laser power of 3.5-4.0 kW with laser travel speed of 16 mm/s and a powder feed rate of 30 g/s. The B material with its higher amount of carbides exhibit a more narrow process window and it is only near 3,5 kW laser power acceptable results can be obtained, while the carbide free C have a slightly lower optimum range at 3,0-3,5 kW.

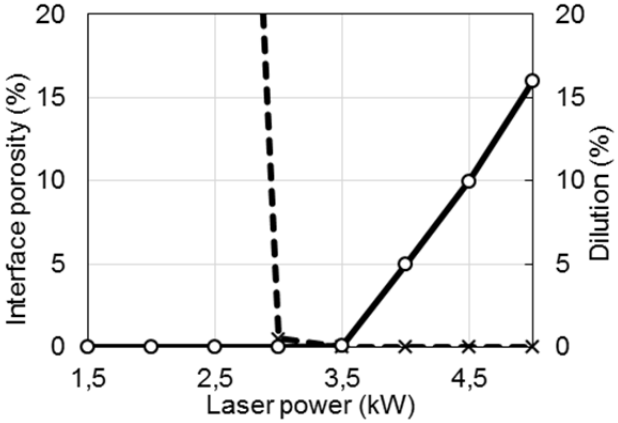


Fig. 1. Process window for material A. Combined diagram of Interface porosity (dashed line) and dilution (solid line). Laser travel speed is 16 mm/s and the powder feed rate is 30 g/min.

The parameters for the cladding of wear samples of material A were selected inside the process window found for the single track clads. A laser power of 3,75 kW, laser travel speed of 16 mm/s and a powder feed rate of 30 g/min was selected. However, using these conditions cracks were found after cladding. In order to decrease the risk for cracks it was decided to pre-heat the plate before cladding to 200 ^{o}C. At the same time the laser power was decreased to 3.4 kW in order to avoid too high dilution. The cladding was performed as patches of approximately 30 mm x 100 mm. Three or four such patches fitted onto one plate. The temperature of the plate was measured before the cladding of each patch. If the temperature was above 300 ^{o}C the cladding was delayed until, the temperature had dropped below 250 ^{o}C.

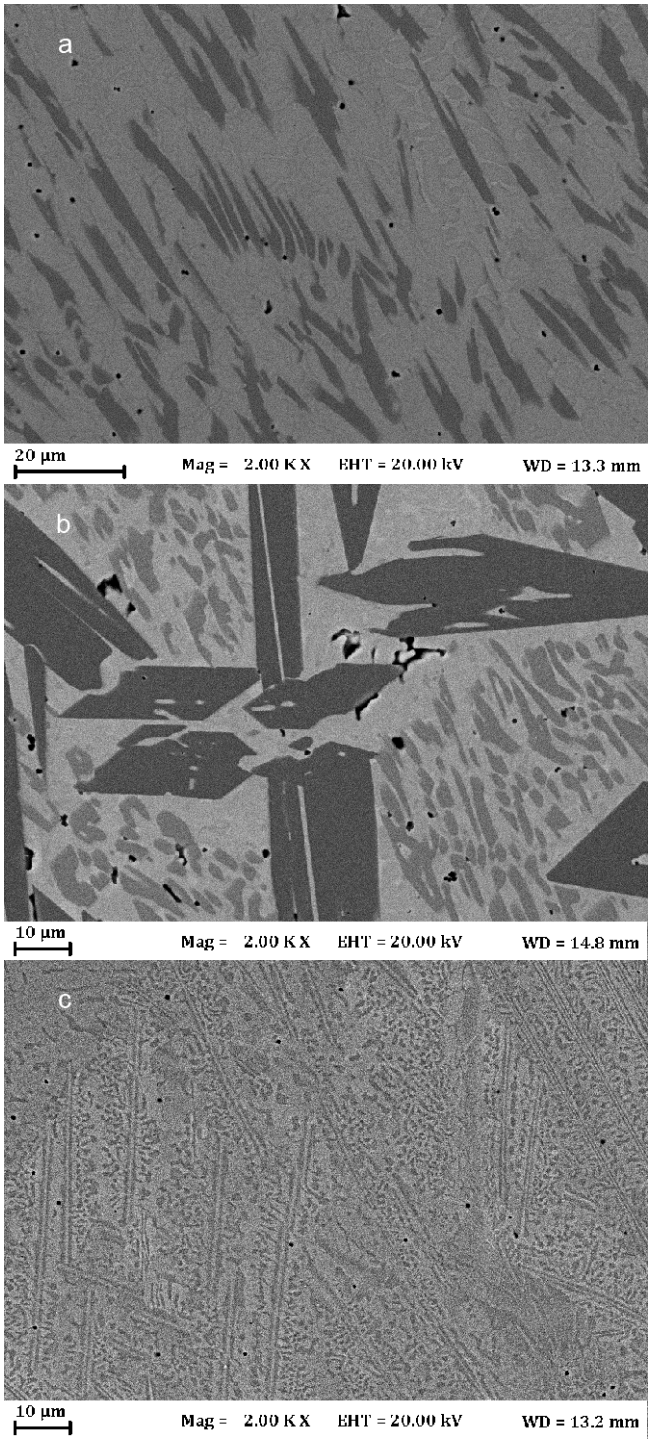


Fig. 2. Scanning electron microscopy of materials a) A, b) B, and c) C. Backscattered electron image.

For the material B it turned out to be necessary to place a buffer layer (Material C) followed by pre-heating to 300 ^{o}C in order to completely avoid cracks. Both layers were clad using a laser power of 3,0 kW. Material C did not require any pre-heating and was clad at a laser power of 3,0 kW. A laser travel speed of 16 mm/s and a powder feed rate of 30 g/s was maintained for all these materials.

In the microstructure of the A material carbides can be found as the dark phase in Fig**.** 2a. The matrix consists of two phases, presumably Ni_3Al and NiAl. Furthermore, small black spots can be found, possibly graphite. The hardness is 570 HV5. The B material with its higher carbon and chromium content exhibits two types of carbides. The darker carbide is presumably Cr_3C_2 while the lighter phase is probably M_7C_3. The matrix also consists of two phases even if it is not evident in Fig**.** 2b. Furthermore, black spots can be seen that are possibly porosity or carbon/graphite. The carbide free material, C exhibit a very fine structure with only two phases, again most likely Ni_3Al and NiAl. The hardness is 900 HV5. The microstructure of material C consists of two phases, also in this case most likely Ni_3Al and NiAl. It solidified in a cell structure or as dendrites depending on the position in the clad. The hardness is 360HV5.

The piston ring / cylinder liner wear contact can be modelled for wear testing in different ways and at different complexity levels. Investigation presented in this paper focuses on a basic ranking of dry sliding friction and wear of three novel prototype materials for piston rings. Therefore, a model wear test of lowest complexity level with so called primitive body geometries is to be used. All other aspects of the piston ring to cylinder liner contact except material and dry sliding are to be intentionally excluded. Selection of test sliding velocities and normal loads will illustrate wear mechanisms under failed oil film lubrication and slight overloads. The test sliding velocities are to be 0.045, 0.13, 0.42, 1.1 and 2.9 m/s. The normal loads are to be 6 and 52 N corresponding max. Herztian contact pressures of 170 respectively 340 MPa. The five test sliding velocities and the two load levels means that wear mapping technique is to be used. As Bowden [] commented it I 1950', the wear mapping is a very opportune way avoid risks with localized presentation of wear data.

The block on ring setup was selected as the most suitable tribological test here for two main reasons: an appropriate scale of contact stresses and wear track as well as convenience of the specimen manufacture. Dry sliding wear applications usually do not belong to highly loaded/concentrated tribological contacts, and the relatively low contact pressure levels in block-on-ring setups will provide a convenient size of wear track. In addition, laser cladding technology can, without high complexity, deposit plain steel bars, from which rectangular test blocks are manufactured using as common chip machining and finishing by plain grinding..

However, in the present case, it was decided to use Tarkalloy-C, a grey cast iron used for cylinder liners in the marine diesel engines that are the target of this investigation. The rings were crowned in order to accommodate any misalignment present in the contact.

In order to be able to compare the performance of the nickel aluminide / chromium carbide materials to relevant reference materials tests were also performed using blocks of nickel aluminide without

carbide (C), cast iron taken from piston ring segments. The tested materials are summarized in Table 2.

Table 2. Material systems used in the dry-sliding adhesive wear test.

Test	Block	Ring
A	Nickel aluminide / 25% Chromium carbide	Cast Iron (Tarkalloy-C)
B	Nickel aluminide / 50% Chromium carbide	
C	Nickel aluminide	

The wear tests were performed on a multi-purpose friction and wear tester – tribometer (Phoenix Tribology TE53). Fig. 3 illustrates the block on ring tribometric test setup. A test block press the block cladded face onto a rotated crowned counter ring. The normal load on the block (F_n) comes from a specimen holder and a load arm assembly with dead weights. A linear displacement transducer (LVDT) registers the total linear wear and a load cell measures the friction force (F_f) in the block on ring contact. Compendx software controls all tribometer sub-systems, log target and acquired values of all test parameters and save in a data file.

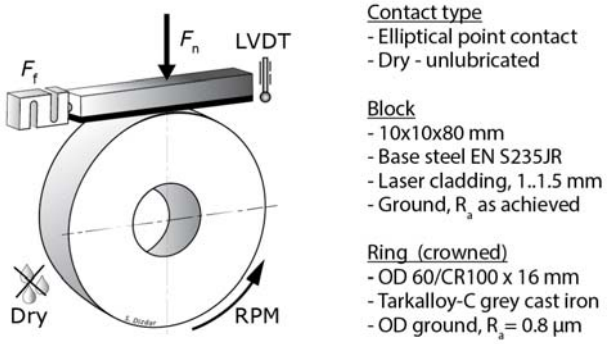


Fig. 3. Block on ring tribometric test setup.

3. Results

The main result are wear mechanism maps shown in Fig. 4. The wear mechanisms were decided based on friction coefficient, wear rate and appearance of the wear surface. – All three wear mechanism maps show wear mechanism regions in principal agreement with those for dry sliding steel to steel contacts [17]. Plasticity dominated wear prevails at low to moderate sliding velocities while oxidational wear occur at relatively high sliding velocities. However, there are substantial differences in friction and wear behavior between the tested materials.

In Test A (material A) exhibit good friction and wear performances, for both 6 and 52 N test normal loads and all five test sliding velocities, see Fig. 4. Friction coefficient is about 0.4-0.6 for the plasticity dominated wear region and drops to about 0.4-0.45 in the oxidational wear region. Wear rate is at 10^{-6} mm^3/Nm level for normal load of 6 N, for both wear regions. At 52 N in normal load, the wear rate is at 10^{-5} mm^3/Nm level in plasticity dominated wear region and drops to 10^{-6} mm^3/Nm in oxidational wear region.

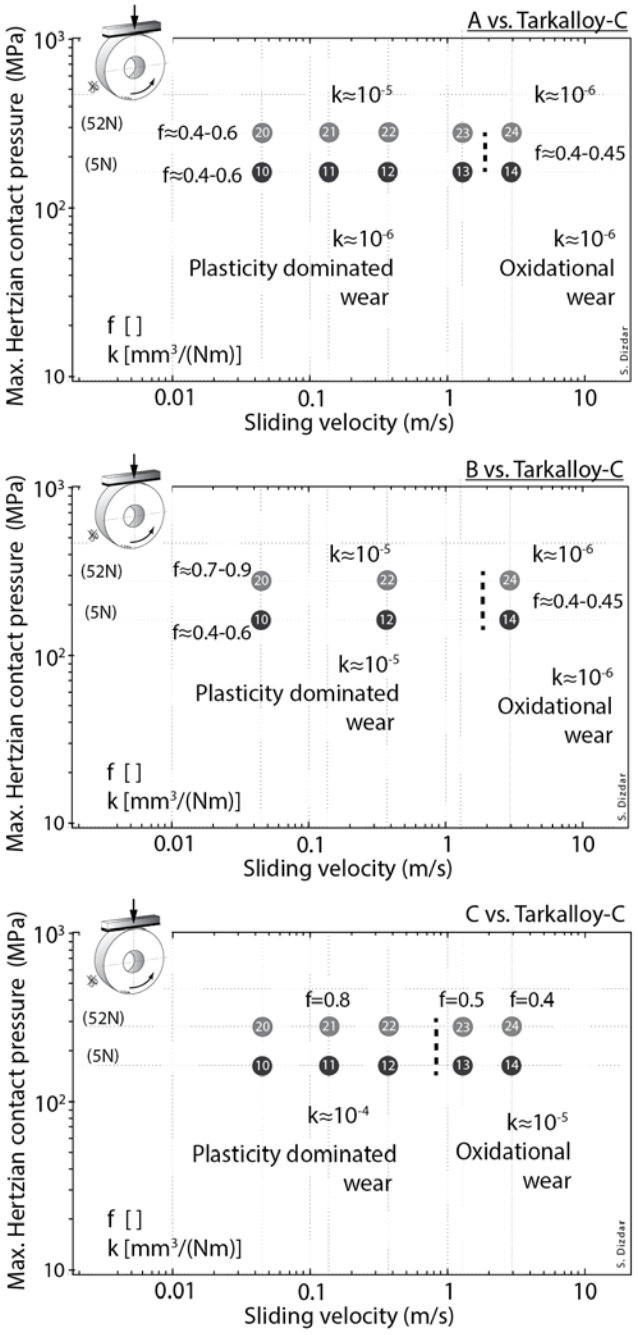


Fig. 4. Wear maps for the tested materials.

Test B (material B) was run as a reduced map including sliding velocities 0.045, 0.37 and 2.9 m/s and it showed a somewhat different behavior, see Fig. 4. Already in the as-ground state the surface is different in that it seems like particles have fallen off, effectively forming small craters, see Fig. 5. However, the size of these craters is quite small about 10 µm. At the lower load of 6 N the coefficient of friction was fairly constant near 0.5 for all three sliding velocities. However, at the higher load the coefficient of friction continuously increased from the start of the test at about 0.3 to about 0.9 at 0.045 mm/s sliding velocity. At the intermediate sliding velocity (0.37 m/s) the behavior was similar, except that the maximum

coefficient of friction was 0.7. It also showed some evidence of material falling off, possibly after formation of a heavily worked surface zone. At the highest sliding velocity the oxidational wear mechanism exhibit basically the same coefficient of friction and wear behavior as at the lower load.

In test C (material C) the friction coefficient is high (0.7-0.9) for high (52 N) loads up to a sliding velocity of 0.37 m/s, the region were plasticity dominated wear dominates, see Fig. 4. At low (6 N) loads the friction coefficient is low (0.4-0.6). At 1.1 m/s the coefficient of friction drops to about 0.5-0.6 at the higher load and remains at 0.4-0.5 for the lower load. At the highest sliding speed at 2.9 m/s the coefficient of friction dropped further to 0.4-0.5 at the higher load and to 0.4 for the lower load.

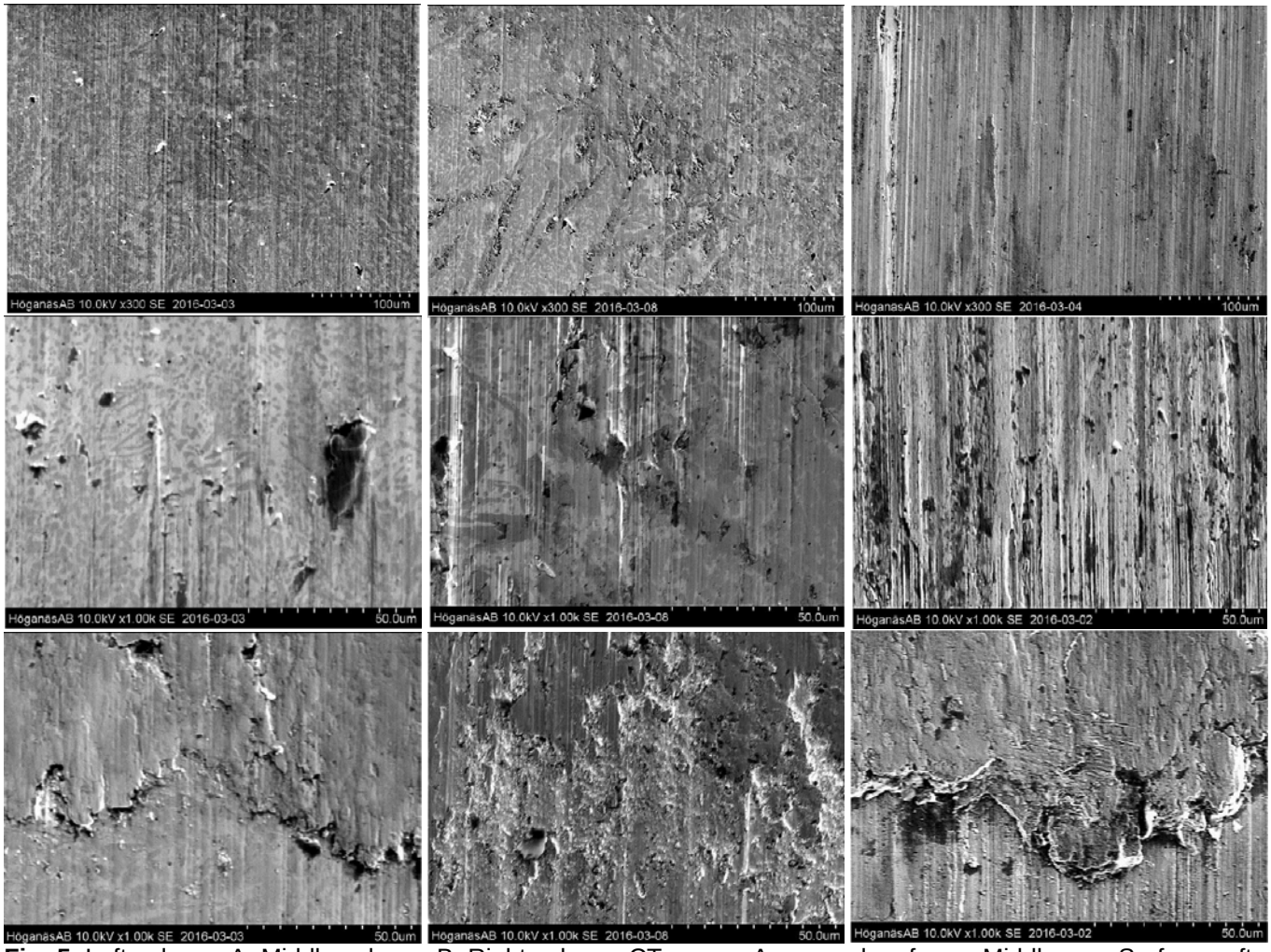


Fig. 5. Left column: A, Middle column: B, Right column: CTop row: As ground surfaces. Middle row: Surfaces after test at sliding speed 0.37 m/s and 6 N normal load. Lower row: Surfaces after test at sliding speed 2.9 m/s and 52 N normal load.

4. Discussion

The carbide free material, C, exhibited very good laser cladding performance. The processing window was relatively wide and no cracks were formed in any of the coupons produced. This indicates some degree of ductility as was expected from literature [14] at this hardness (370 HV_5).

Laser cladding of the powder with the highest carbide content, B, proved to be quite difficult without forming cracks. Pre-heating alone did not provide a solution to avoiding cracks in all cases. The wear samples used in the investigation required both pre-heating and the use of a buffer layer using the carbide free nickel aluminide powder (C). The volume fraction of hard phase is about 50% for this material and most of it is precipitated in the melt. A consequence of this is that the melt pool will have very poor fluidity and that there is a risk for solidification porosity. The observed black spots may be porosity, Fig. 2c. A further consequence is that the accommodation of the residual stresses due to the large temperature drop will be limited since it is only 50% of the material, the matrix, which can plastically deform. At room temperature this is manifested in the very high hardness (900 HV_5) exhibited by this material.

Material A is a good compromise between B and C. It has approximately half of the volume fraction carbide found in B. It gives a significant hardness increase

over C, 600 compared to 370 HV_5, but still have a sufficient amount of matrix phase (~75%) to accommodate the residual stresses formed. When cladding using this material, the tendency to form cracks was much less prominent. Depending on the coating size it was sometimes possible to perform the cladding operation without pre-heating the substrate.

In the wear testing all the tested materials exhibit a plasticity dominated wear mechanism for sliding speeds from 0.045 m/s up to about 1.1 m/s. At higher sliding speeds the wear mechanism is dominated by oxidative wear.

Nickel aluminide material without the carbide (C) exhibits poor behavior in the plasticity dominated region with very high coefficient of friction, 0.7-0.9, and a high wear rate of 10^{-4} mm^3/Nm while performance recovers somewhat in the oxidative wear dominated region were coefficient of friction drops to about 0.4 and wear rate to 10^{-5} mm^3/Nm [17].

However, the introduction of the carbide into the nickel aluminide system provides several advantages. The most significant, for the intended application, is the improvement in wear behavior at low speed. Here apparently the carbides prevent adhesive junctions so that coefficient of friction can remain relatively low and that the wear rate for the carbide containing material is lower at all speeds and loads tested.

The carbide containing material (A) exhibits a coefficient of friction of 0.4-0.6, and a wear rate of 10^{-6} mm^3/Nm in the plasticity dominated region and 0.4-0.45 respective 10^{-6} mm^3/Nm in the oxidative wear dominated region.

The material with a higher carbide content (B) performs well at the low load conditions, but at high loads and low speeds, the coefficient of friction is 0.7-0.9. The expected better wear performance may be offset by the fact that it appears that material is falling out forming small craters on the wear surface, Fig. 5. Carbides falling out will create craters and also scratch the surface resulting in increased surface roughness and increased wear rate.

The piston ring to cylinder liner contact has, as previously mentioned, a risk for severe wear in the piston top dead center position where full film lubrication cannot be established due to low sliding velocity and other factors. Here, the wear resistance is provided by friction and wear reducing surface phases. Carbides in nickel aluminide alloy A and B have been showed here to reduce both friction and wear in dry sliding conditions at low sliding velocities in comparison to carbide free nickel aluminide alloy C.

5. Conclusions

The nickel aluminide alloy A with 25% carbides has been showed here to reduce both friction and wear in dry sliding conditions at low sliding velocities in comparison to carbide free nickel aluminide alloy C.

6. References

[1] Woodyard, D. Exhaust Emissions and Control. *Pounder's Mar. Diesel Engines Gas Turbines* 61–86 (2009). doi:10.1016/B978-0-7506-8984-7.00003-5

[2] Liu, Y. Q., Du, J. Z., Tan, P. Q. & Du, A. M. Progress on Denitration and Desulfuration Technologies for Marine Diesel Engines. *Appl. Mech. Mater.* **713–715,** 51–56 (2015).

[3] Cheng, H. S. in *ASM Handbook, Vol 18* 88–97 (ASM International, 1992).

[4] Brenneke, A. M. *Chrome plated piston rings design and application*. *SAE Technical Paper 490113* (1949). doi:10.4271/490113.

[5] Rastegar, F. & Richardson, D. E. Alternative to chrome: HVOF cermet coatings for high horse power diesel engines. *Surf. Coatings Technol.* **90,** 156–163 (1997).

[6] Aram, M. Thermal Spryaing of a Piston Ring. *US 2005/0073107 A1* **1,** (2005).

[7] Obara, R., Takiguchi, K. & Hosotsubo, Y. Piston rings and thermal spray coating used thereiin, and method for manufacturing thereof. *US 7291384 B2* **2,** (2007).

[8] Hwang, J.-H., Han, M.-S., Kim, D.-Y. & Youn, J.-G. Tribological Behavior of Plasma Spray Coatings for Marine Diesel Engine Piston Ring and Cylinder Liner. *J. Mater. Eng. Perform.* **15,** 328–335 (2006).

[9] Picas, J. A., Forn, A. & Matthäus, G. HVOF coatings as an alternative to hard chrome for pistons and valves. *Wear* **261,** 477–484 (2006).

[10] Yan, J., He, Z., Wang, Y., Qiu, J. & Wang, Y. Microstructure and Wear Resistance of Plasma-Sprayed Molybdenum Coating Reinforced by MoSi2 Particles. *J. Therm. Spray Technol.* **25,** 1322–1329 (2016).

[11] Stoloff, N. S., Liu, C. T. & Deevi, S. C. Emerging applications of intermetallics. *Intermetallics* **8,** 1313–1320 (2000).

[12] Yang, J.-M., Kao, W. H. & Liu, C. T. Development of Nickel aluminide matrix composites. *Mater. Sci. Eng. A* **107,** 81–91 (1989).

[13] Samuelsson, P., Gong, K., Li, C. & Aram, M. Piston ring having wear resistant composition. *US7052018B2* (2006).

[14] Deevi, S. C. & Sikka, V. K. Nickel and iron aluminides: an overview on properties, processing, and applications. *Intermetallics* **4,** 357–375 (1996).

[15] Velon, A. Oxidation of Fe- and Ni-aluminides in dry and humid atmospheres. *Dissertation: Chalmers University of Technology* (Chalmers University of Technology, 2001).

[16] Bengtsson, S. New powder composition and use thereof. *WO 2016/146735 A1* (2016).

[17] Lim, S. C. & Ashby, M. F. Overview no. 55 Wear-Mechanism maps. *Acta Metall.* **35,** 1–24 (1987).